

See discussions, stats, and author profiles for this publication at: <https://www.researchgate.net/publication/11665902>

# Three-Dimensional Structure of a Purple Lipxygenase

ARTICLE *in* JOURNAL OF THE AMERICAN CHEMICAL SOCIETY · DECEMBER 2001

Impact Factor: 12.11 · DOI: 10.1021/ja011759t · Source: PubMed

---

CITATIONS

109

---

READS

25

5 AUTHORS, INCLUDING:



**Ewa Skrzypczak-Jankun**

University of Toledo

**112** PUBLICATIONS **2,817** CITATIONS

SEE PROFILE



**William Richard Dunham**

University of Michigan

**134** PUBLICATIONS **3,748** CITATIONS

SEE PROFILE

## Three-Dimensional Structure of a Purple Lipoxygenase

Ewa Skrzypczak-Jankun,\* Rebecca A. Bross, Richard T. Carroll, Willam R. Dunham, and Max O. Funk, Jr.\*

Contribution from the Department of Chemistry and Medicinal and Biological Chemistry, University of Toledo, 2801 West Bancroft Street, Toledo, Ohio 43606

Received July 19, 2001

**Abstract:** Polyunsaturated fatty acid metabolism is governed primarily by two enzymes, prostaglandin H synthase and lipoxygenase. The crystal structure of the metastable product-oxidized purple form of soybean lipoxygenase-3 was determined at 2.0 Å resolution. The data reveal that the chromophore corresponds to an iron-peroxide complex, a potential intermediate in the catalyzed reaction. A significant alteration of the iron site accompanies the formation of the complex. The structure, the first for a fatty acid-lipoxygenase complex, also reveals an unexpected mode of binding, and identifies amino acid residues that may play significant roles in catalysis, regio- and stereoselectivity.

### Introduction

Polyunsaturated fatty acid metabolism is governed by two enzymes, cyclooxygenase and lipoxygenase. Together they are responsible for the inauguration of the biosynthesis of a host of metabolites known collectively as eicosanoids.<sup>1</sup> The discovery that these compounds play pivotal roles in diseases that include an inflammatory component has given rise to a substantial research effort to elucidate the structure and mechanism of action of these key biosynthetic enzymes. Structure/function studies of cyclooxygenase have culminated in the discovery of numerous inhibitors with therapeutic potential, the nonsteroidal antiinflammatory drugs.<sup>2</sup> Parallel investigations into the structure of lipoxygenase and its complexes with small molecules, e.g. substrate, product, and inhibitors, for the generation of therapeutically useful compounds have not reached the same level of development. Lipoxygenase catalysis depends on the participation of a unique non-heme iron cofactor.<sup>3</sup> The enzyme activates the substrate polyunsaturated fatty acid toward combination with molecular oxygen by a hydrogen atom abstraction reaction. The results of kinetic isotope effect experiments implicate a tunneling mechanism for this key step in the catalyzed reaction.<sup>4</sup> How the enzyme perpetrates the transformation in this way is consequently also a matter of considerable fundamental interest in chemistry.

Several crystallographically determined structures of lipoxygenases (two isoforms from soybeans and one from rabbit) have been reported.<sup>5–8</sup> The proteins share an overall folding pattern and contain very similar non-heme iron sites. The only

significant difference in the iron amino acid ligands is that in the rabbit enzyme one of the iron coordination positions is occupied by histidine, while the structures of the soybean enzymes contain asparagine in the same location, but at just beyond a bonding distance. The structures of all of the complexes of these two enzymes determined to date identify the same site for ligand binding adjacent to the non-heme iron.<sup>8–10</sup>

All of the crystallographically determined structures for lipoxygenases up to now, however, have been conducted on the native, sometimes called resting, iron(II) enzyme. Activation for catalysis requires oxidation of the cofactor, and catalysis depends on its redox cycling.<sup>11</sup> The only known oxidant for this reaction is the lipid hydroperoxide product of the catalyzed reaction.<sup>12</sup> The oxidation of lipoxygenase to its active, iron(III) form is accompanied by characteristic spectroscopic changes. For example, treatment of solutions of the native enzyme with 1 equiv of hydroperoxide product produces a slightly yellow color, and the samples exhibit EPR signals that are characteristic of high-spin iron(III).<sup>13</sup> The EPR spectrum reflects an iron environment that is not strictly homogeneous. Combinations of signals ranging from mostly axial in nature to purely rhombic have been obtained under different experimental conditions. The contributions vary, for example, with pH and the presence or absence of low molecular weight alcohol in the sample.<sup>14</sup> When solutions of soybean lipoxygenase-1 are treated with more than 1 equiv of the peroxide product, a distinct purple color is obtained. The purple form of the enzyme also contains high-spin iron(III) in multiple environments judging from the features of the observed EPR spectrum.<sup>15</sup> Solutions of purple soybean

\* Address correspondence to these authors: E.S.J. (ejankun@protein.wu.toledo.edu) or M.O.F. (mfunk@uoft02.toledo.edu).

(1) Prescott, S. M. *J. Biol. Chem.* **1999**, *274*, 22901.  
 (2) Dannhardt, G.; Kiefer, W. *Eur. J. Med. Chem.* **2001**, *36*, 109–126.  
 (3) Solomon, E. I.; Brunold, T. C.; Davis, M. I.; Kemsley, J. N.; Lee, S. K.; Lehnert, N.; Neese, F.; Skulan, A. J.; Yang, Y. S.; Zhou, J. *Chem. Rev.* **2000**, *100*, 235–349.  
 (4) Ridkert, K. W.; Klinman, J. P. *Biochemistry* **1999**, *38*, 12218–12228.  
 (5) Boyington, J. C.; Gaffney, B. J.; Amzel, L. M. *Science* **1993**, *260*, 1482–1486.  
 (6) Minor, W.; Steczko, J.; Stec, B.; Otwinowski, Z.; Bolin, J. T.; Walter, R.; Axelrod, B. *Biochemistry* **1996**, *35*, 10687–10701.  
 (7) Skrzypczak-Jankun, E.; Amzel, L. M.; Kroa, B. A.; Funk, M. O. *Protein Struct. Funct. Genet.* **1997**, *29*, 15–31.  
 (8) Gillmor, S. A.; Villaseñor, A.; Fletcher, R.; Sigal, E.; Browner, M. F. *Nature Struct. Biol.* **1997**, *4*, 1003–1009.

(9) Pham, V. C.; Jankun, J.; Skrzypczak-Jankun, E.; Flowers, R. A., II; Funk, M. O. *Biochemistry* **1998**, *37*, 17952–17957.

(10) Skrzypczak-Jankun, E.; Pham, V. C.; Flowers, R. A.; Jankun, J.; Funk, M. O. American Crystallographic Association Annual Meeting, Arlington, VA, July 18–23, 1988; p 99, P040.

(11) Funk, M. O.; Carroll, R. T.; Thompson, J. F.; Sands, R. H.; Dunham, W. R. *J. Am. Chem. Soc.* **1990**, *112*, 5375–5376.

(12) Haining, J. L.; Axelrod, B. *J. Biol. Chem.* **1958**, *232*, 193–202.

(13) DeGroot, J. J. M. C.; Veldink, G. A.; Vliegthart, J. F. G.; Boldingh, J.; Wever, R.; VanGelder, B. F. *Biochim. Biophys. Acta* **1975**, *377*, 71–79.

(14) Slappendel, S.; Aasa, R.; Malmstrom, B. G.; Verhagen, J.; Veldink, G. A.; Vliegthart, J. F. G. *Biochim. Biophys. Acta* **1982**, *708*, 259–265.

(15) DeGroot, J. J. M. C.; Garssen, G. J.; Veldink, G.; Vliegthart, J. F. G.; Boldingh, J.; Egmond, M. R. *FEBS Lett.* **1975**, *56*, 50–54.

lipoyxygenase-1 are both thermally unstable and photolabile.<sup>16</sup> An investigation of the photolysis of the purple enzyme concluded that the chromophore represented a catalytically competent species, possibly an iron-peroxide complex, that might be an intermediate in the catalyzed reaction.<sup>17</sup> Working with a different isoform of the soybean enzyme (lipoyxygenase-3) we have been able to obtain crystals of purple lipoyxygenase that persist long enough for X-ray diffraction analysis. The X-ray crystal structure was solved at 2.0 Å resolution by molecular replacement. The structure is the first for an iron(III) lipoyxygenase, and the first example of a lipoyxygenase/fatty acid complex to be determined. The mode of fatty acid binding is therefore evident, and the structure establishes that purple lipoyxygenase is an iron-peroxide complex.

## Results and Discussion

**Purple Lipoyxygenase 3 Is a Metastable Iron-Peroxide Complex.** Titration of a 250 μM solution of lipoyxygenase-3 at pH 8.5 with (9Z,11E)-13(S)-hydroperoxy-9,11-octadecadienoic acid (13-HPOD) produced the UV–visible absorbance spectra presented in Figure 1a. An absorbance maximum centered around 590 nm (1400 L mol<sup>-1</sup>cm<sup>-1</sup>) was obtained. Frozen samples of solutions of the product-treated enzyme were analyzed by EPR spectroscopy (Figure 1b). While the rhombic feature around g4.3 was the most conspicuous signal in each spectrum, the various axial signals around g6 constituted a much greater fraction of the EPR visible iron upon integration. Although the spectroscopic properties of solutions of lipoyxygenase-3 treated with excess 13-HPOD were found to be similar to those reported previously for lipoyxygenase-1, it was our consistent observation that solutions of lipoyxygenase-3 retained their color longer than similarly treated samples of lipoyxygenase-1. For example, it was originally reported that solutions of purple lipoyxygenase-1 lasted only about 1 h at 0 °C.<sup>15</sup> The loss of the purple color correlated with the conversion of 13-HPOD into mainly (9Z)-(trans-12,13-epoxy)-11-hydroxy-9-octadecenoic acid.<sup>18</sup> By contrast, solutions of lipoyxygenase-3 oxidized with excess 13-HPOD retained their color overnight when stored at 4 °C. We sought to capitalize on the enhanced stability of this oxidized isoform by undertaking a resonance Raman spectroscopy investigation of the purple form of lipoyxygenase-3. To our disappointment, but consistent with all previous observations of lipoyxygenase-1, purple solutions of lipoyxygenase-3 were efficiently photobleached in the light path of the Raman spectrophotometer at 2 °C.<sup>17</sup> The behavior of lipoyxygenase-3, while not strictly identical in all respects, was similar to the behavior of lipoyxygenase-1 upon treatment with excess product.

Freshly prepared crystals of lipoyxygenase-3 were treated directly with a solution of 13-HPOD, which caused them to gradually turn purple. The purple crystals were not stable, especially upon photoirradiation. Consequently, the crystals were handled and the data were collected with only the light necessary for mounting and optical alignment. While cryoprotection of crystals might be considered an option, we have found that the change induced in the lipoyxygenase-3 structure upon freezing doubles the number of variables necessary for calculations without any significant gain in the number of observations.<sup>19</sup> Therefore, data were obtained at room temperature in the dark by using three crystals, and the time for data collection was

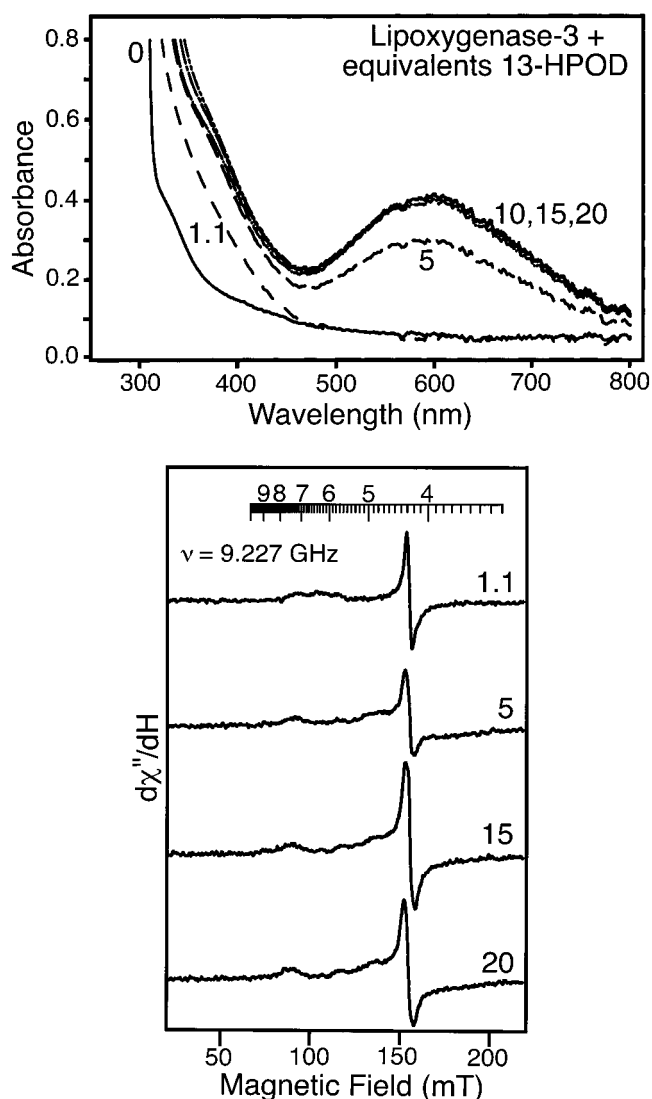


**Figure 1.** Spectroscopic properties of soybean lipoyxygenase-3 treated with excess 13-HPOD: (a) UV–visible spectra for lipoyxygenase-3 (250 μM, 0.1 M TrisHCl, pH 8.5) treated with 13-HPOD in varying ratios and (b) EPR spectra for lipoyxygenase-3 (250 μM, 0.1 M TrisHCl, pH 8.5) treated with 13-HPOD in varying ratios.

held to less than 3 h per crystal. Despite the limitations imposed by the instability of the purple crystals, the data provided clear evidence in the electron density difference map for fatty acid binding within the enzyme central cavity near the iron site. When 13-HPOD was included in the calculations the structure was successfully refined to a discrepancy factor of  $R < 20\%$ . The crystallographic data and refinement statistics are presented in Table 1. Figure 2 shows a stereoview of the final  $2F_o - F_c$  map near the binding site. In the crystal structure, the 13-HPOD molecule forms a covalent complex with iron via the peroxy group. As illustrated in Figure 3, the peroxide occupies the sixth ligand position in the iron coordination sphere producing a slightly distorted octahedral ( $C_{3v}$ ) geometry. The peroxide displaces a water molecule from its position near (4.0 Å) the iron atom in the structure of the native enzyme. Further, coordination of the metal by Asn713 is evident in the structure obtained from the purple crystals in comparison to the situation in the native enzyme, where the residue is situated at a non-bonding distance (3.0 Å). The bond distances and angles for

(16) Nelson, M. J.; Seitz, S. P.; Cowling, R. A. *Biochemistry* **1990**, *29*, 6897–6903.

(17) Nelson, M. J.; Chase, D. B.; Seitz, S. P. *Biochemistry* **1995**, *34*, 6159–6163.

(18) Garssen, G. A.; Veldink, G. A.; Vliegthart, J. F. G.; Boldingh, J. *Eur. J. Biochem.* **1976**, *62*, 33–36.

(19) Skrzypczak-Jankun, E.; Bianchet, M. A.; Amzel, L. M.; Funk, M. O. *Acta Crystallogr.* **1996**, *D52*, 959–965.

**Table 1.** Crystallographic Data and Refinement Statistics

space group	C2
cell dimensions: <i>a</i> , <i>b</i> , <i>c</i> (Å), $\beta$ (deg)	112.65, 137.28, 61.89, 95.56
resolution (Å)	40–2.0
total no. of observation	107634
no. of unique reflcns	48693
completeness	78 (68) <sup>a</sup>
<i>I</i> / $\sigma$	11.5 (1.3)
<i>R</i> <sub>merge</sub> (%)	6.4 (35.2)
<i>R</i> <sub>cryst</sub> (%) (41,035 reflcns, 40–2.0 Å)	19.6
<i>R</i> <sub>free</sub> (%) <sup>b</sup>	29.6
non-hydrogen atoms protein/ cofactor/ligand/water	6697/1/22/529
rms deviations	
bonds (Å)	0.007
angles (deg)	1.4

<sup>a</sup> Values in parentheses are for the highest resolution shell 2.07–2.00 Å. <sup>b</sup> *R*<sub>free</sub> was calculated with a test set containing 10% of the data.

the iron coordination sphere are collected in Table 2. While there are two excellent recent examples of small molecule models for the purple iron(III) peroxide complex in lipoxigenase, crystals of the complexes were not obtained due to instability.<sup>20,21</sup> Solutions of these model complexes were characterized by electronic absorption, EPR, and resonance Raman spectroscopy and electrospray ionization mass spectrometry. The solutions displayed absorption and EPR spectra similar to those obtained for product-oxidized solutions of lipoxigenase. Distinctive absorption bands in the resonance Raman spectra were assigned to both O–O and Fe–O stretching modes. The data were thus consistent with the formation of an end-on alkylperoxo iron(III) complex and the absorption bands near 600 nm for these complexes were assigned to the alkylperoxo to iron(III) charge-transfer transition. Resonance Raman data for the purple form of lipoxigenase have been difficult to obtain (*vide supra*). However, the crystallographic data reported here provide the first structural verification for any mononuclear non-heme iron-peroxide complex. The data are consistent with all of the previously reported spectroscopic observations on this form of the enzyme and also with the characteristic features of the model complexes, providing a coherent view of the structure and bonding in the purple species.

**The Lipoxigenase–Fatty Acid Interaction.** Considering the similarities in the catalyzed reactions, the structural features of fatty acid complexes of cobalt-substituted ovine cyclooxygenase-(Co<sup>3+</sup>-oPGHS-1)<sup>22</sup> and lipoxigenase are remarkably different. Cyclooxygenase is a heme protein, and arachidonic acid binds ~15 Å from the metal cofactor measured from Co<sup>3+</sup> to C13 of the fatty acid. The redox chemistry is apparently mediated by an intervening tyrosine residue (Tyr385). The fatty acid binds with its carboxylate end at the opening of a channel in the protein, anchored by interactions with Arg120 and Tyr355, and adjacent to the unique membrane binding domain of cyclooxygenase. The arachidonic acid molecule extends into the COX channel past Tyr385 into a pocket lined with hydrophobic residues. In an inactive mutant, however, it binds in the same location, but in the reverse orientation.<sup>23</sup> By contrast lipoxigenase binds the fatty acid ligand immediately adjacent to the non-heme iron site, completely enveloped in internal channels of the protein.

Beyond the identification of the binding sites, the structures reveal the orientations of the fatty acids, and have the potential to disclose the aspects of the enzymes responsible for the features of the catalyzed reactions, e.g., mechanism of action and stereospecificity. For example, the orientation of arachidonic acid in the Co<sup>3+</sup>-oPGHS-1 complex is consistent with many features of the catalyzed reaction providing reinforcement for the current working hypothesis for the enzyme mechanism: stereospecific hydrogen atom abstraction, stereospecific reactions with oxygen molecules, and the stereospecific peroxy radical cyclization reaction.<sup>23</sup> With lipoxigenase, it is not yet completely clear how the enzyme controls the regioselectivity and stereoselectivity of catalysis, and what factors govern the outcome of the peroxidation reaction and the formation of possible products. Soybean lipoxigenase isozymes (lipoxigenase-1 and lipoxigenase-3) provide an interesting study in contrast since their mechanisms lead to both single (lipoxigenase-1) and multiple (lipoxigenase-3) products of 9/13 peroxidation of linoleic acid. Further, the products can be produced either with a high degree of stereoselectivity (lipoxigenase-1) or with similar contributions of *R* and *S* chirality (lipoxigenase-3). Recent site directed mutagenesis experiments with lipoxigenase-1 suggest that steric restraints placed on the approach of oxygen to the enzyme-bound substrate by the surrounding amino acid side chains culminate in the observed stereo- and regioselectivity.<sup>24</sup> Replacing bulky leucine residues at positions 546 and 754 in lipoxigenase-1 (corresponding to 565 and 773 in lipoxigenase-3) with the less demanding alanine resulted in less of the 13-substitution product, more of the 9-isomer, and a lower level of stereoselectivity at both positions. The amino acids at these positions cannot, however, by themselves account for the differences observed in the product distributions of the isoenzymes, as they are conserved in the two proteins. The present report provides the first evidence on this subject from an X-ray analysis of lipoxigenase-3 in complex with the product of the catalyzed reaction.

The 13-HPOD molecule anchors its carboxyl group to the hydrophilic residues OG Ser510 and NH2 Arg726, and via water molecules to O Gln716, OD2 Asp766, and O Gly720 (Figure 4). Binding of 13-HPOD does not disrupt the Asp509-Arg726 salt bridge. The 9-*cis*, 11-*trans* double bond system has His518-Trp519 on one side and hydrophobic residues Leu565, Ile572, and Leu773 on the opposite side in the immediate vicinity. The aliphatic end of the molecule, C14–C18, is squeezed between Ile857 and Leu277 protruding into a hydrophobic channel. The channel comes to an end at the interface between the two domains making it easily accessible to the solvent. The electron density map (Figure 2) shows no density for the C17–C18 end of 13-HPOD. The hydrophobic channel is lined by the side chains of Leu273, Thr274, Leu277, Leu560, Ile557, Ile857, and Ile772, which allows for more than one conformation for the aliphatic substituent.

A comparison of the structures of native lipoxigenase-3 and the complex shows surprisingly few differences, either in the protein or the solvent. Superposition of all residues of these two structures gives a root-mean-square deviation of 0.4 Å. The only amino acid dislocated in a significant way from its original place is Gln514 (Figure 5), which in the native enzyme participates in a hydrogen bonding network connecting ND1

(20) Wada A.; Ogo S.; Watanabe Y.; Mukai M.; Kitagawa T.; Jitsukawa K.; Masuda H.; Einaga H. *Inorg. Chem.* **1999**, *38*, 3592–3593.

(21) Kim, J.; Zang, Y.; Costas, M.; Harrison, R. G.; Wilkinson, E. C.; Que, L. *J. Biol. Inorg. Chem.* **2001**, *6*, 275–284.

(22) Malkowski, M. G.; Ginell, S. L.; Smith, W. L.; Garavito, R. M. *Science* **2000**, *289*, 1933–1937.

(23) Kiefer, J. R.; Pawlitz, J. L.; Moreland, K. T.; Stegman, R. A.; Hood, W. F.; Gierse, J. K.; Stevens, A. M.; Goodwin, D. C.; Rowlinson, W. W.; Marnett, L. J.; Stallings, W. C.; Kurumbail, R. G. *Nature* **2000**, *405*, 97–101.

(24) Knapp, M. J.; Seebeck, F. P.; Klinman, J. P. *J. Am. Chem. Soc.* **2001**, *123*, 2931–2932.



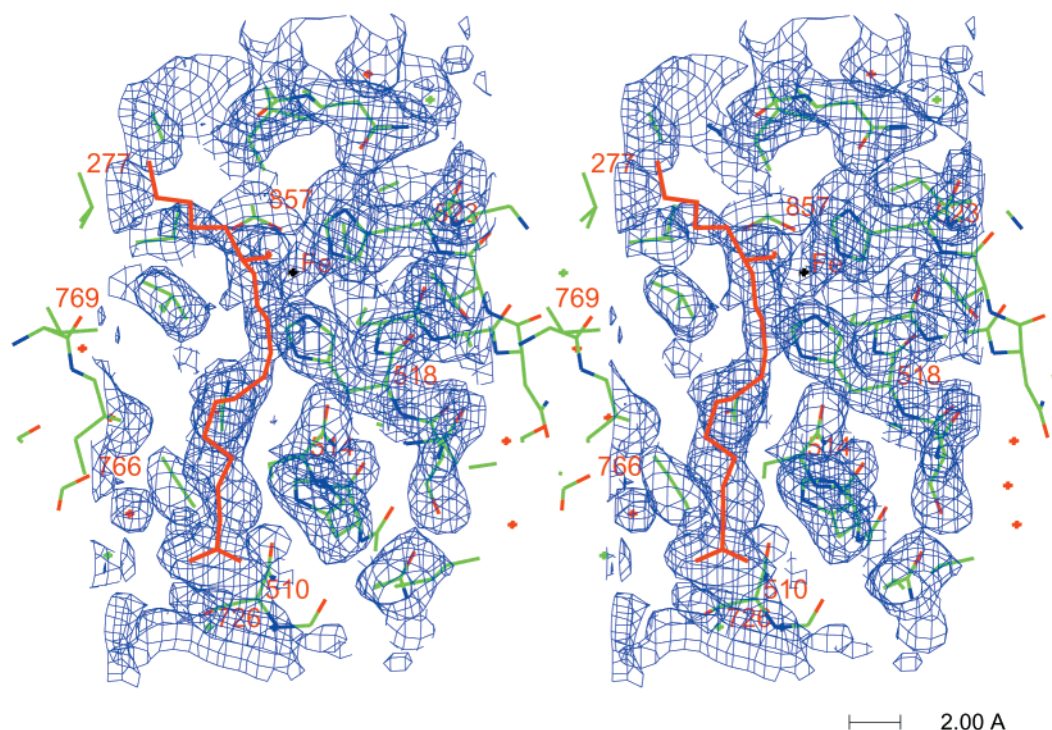


**Figure 2.** Stereoview of the 13-HPOD binding site showing the final  $2F_o - F_c$  map ( $1\sigma$  contouring level) and selected residue numbers.

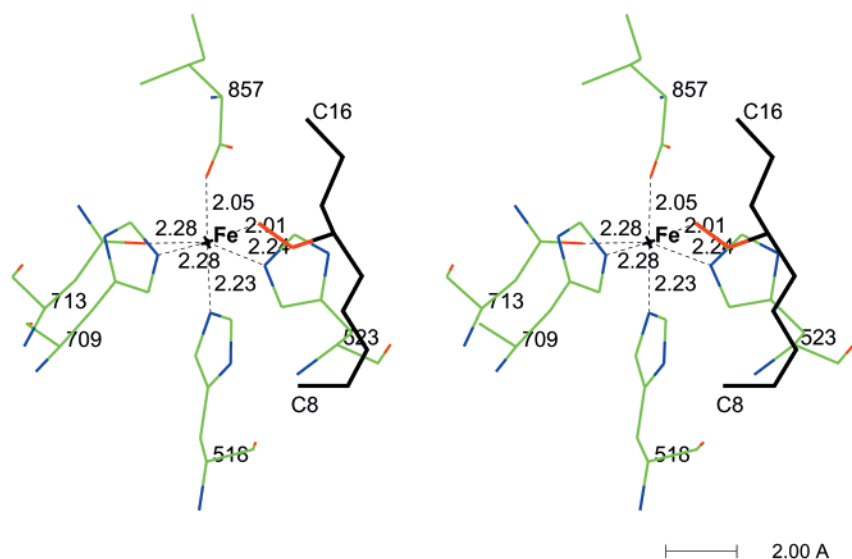


**Figure 3.** The iron site with bound 13-HPOD. The ends of 13-HPOD have been omitted for clarity.

His518...OE1 Gln514, NE2 Gln514...OE1 Gln716, NE2 Gln716...OD1 Asn713, and ND2 Asn713...O Leu773. Atoms C5–C6–C7 from the fatty acid occupy the place taken up by the Gln514 side chain in the native enzyme, with C5 only 2.9 Å away from OE1 Gln716. The maps show residual electron density where Gln514 would be in the native protein, and so our conclusion is that this side chain is disordered. The observation of different orientations for the Gln514 side chain could be the basis for an explanation for the lack of regioselectivity in lipxygenase-3 catalysis. If Gln514 had remained in its original hydrogen bonding network, the passage for the carboxyl end of the fatty acid would be blocked. If the carboxyl group of a fatty acid substrate could be stabilized by an interaction with the hydrogen bonding network around Gln514, employing water molecules and possibly Asp766, this would bring the C9 atom instead of the C13 atom from the fatty acid near the iron cofactor during the catalyzed reaction. In the present experiments the compound

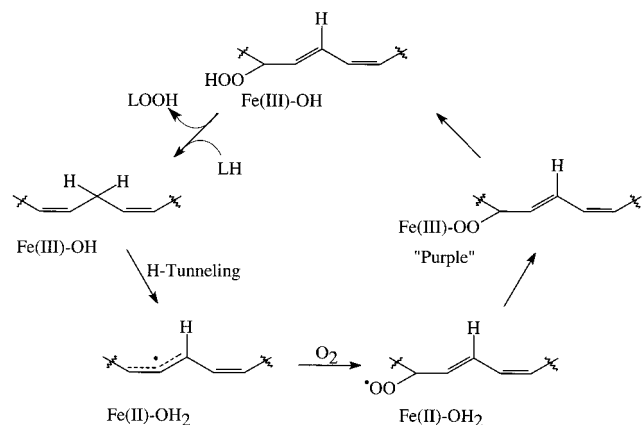
was already oxidized at the 13 position, and the displaced Gln514 can be stabilized in its new location by bifurcated hydrogen bonds between NE2 Gln514 and SG Cys511, O Cys511. The observed turn of SG in the direction of Gln514 and the small shift in the position of the Leu515 side chain support this conclusion. Incorporation of 13-HPOD into this space in the molecule also dislocates solvent molecules, but only two of them (Wat936 and Wat901 in the native lipxygenase-3 structure).

The binding site in general appears to be more flexible in lipxygenase-3 than in lipxygenase-1 as a consequence of amino acid differences in the aligned sequences (lipxygenase-1/lipxygenase-3): Ser747/Asp766, Thr756/Arg775, and Glu256/Thr274 (Figure 5). For example, Asp766 participates in the hydrogen bonding network that holds the carboxyl group of 13-HPOD in place. However, it could also form a salt bridge with an alternate rotamer of Arg726 that was clearly visible in the

**Table 2.** Iron Coordination: Distances (Å) and Angles (deg)

atoms (L3 numbering)	native		lipoxygenase-3 13-HPOD (2.0 Å) [room temp] 13S (13.7)
	lipoxygenase-1 (1.4 Å) <sup>a</sup> [100 K]	lipoxygenase-3 (2.6 Å) [room temp]	
Fe-NE2 His518	2.23	2.23	2.23
Fe-NE2 His523	2.26	2.21	2.24
Fe-NE2 His 709	2.21	2.26	2.28
Fe-OD1 Asn713	3.05	3.01	2.28
Fe-OXT Ile857	2.40	2.13	2.05
Fe-O22 <sup>b</sup> 13HPOD 859	2.56 (Wat842)	4.02 (Wat901)	2.01 (2.05)
518NE2-Fe-523NE2	95.2	91.6	84.5
518NE2-Fe-709NE2	102.3	100.7	98.9
523NE2-Fe-709NE2	105.9	86.5	89.2
857OXT-Fe-713OD1	95.6	106.6	103.4
857OXT-Fe-O22	95.6	99.9	88.4 (81.1)
713NE2-Fe-O22	66.4	109.3	102.9 (113.1)
518NE2-Fe-713OD1	74.9	67.8	77.9
518NE2-Fe-O22	86.3	76.8	90.1 (97.2)
523NE2-Fe-857OXT	91.5	94.5	94.3
523NE2-Fe-O22	97.5	69.4	82.7 (74.3)
709NE2-Fe-713OD1	91.9	91.5	87.9
709NE2-Fe-857OXT	86.4	85.5	82.4
518NE2-Fe-857OXT	167.1	171.6	178.2
523NE2-Fe-713OD1	161.2	158.6	161.5
709NE2-Fe-O22	154.0	155.6	167.3 (155.7)

<sup>a</sup> Data resolution in parentheses. <sup>b</sup> For this table it is assumed that the place in the coordination sphere filled by O22 from 13-HPOD (PDB 1IK3, A13S, and B13R) is occupied by water 842 in native lipoxygenase-1 (PDB 1YGE) and water 901 in native lipoxygenase-3 (PDB 1LNH).

**Scheme 1**

density map of the native enzyme.<sup>7</sup> A reorientation of Arg726 would support the hydrogen bonding network around Gln514•••Gln716 with Asp766•••Arg726•••H<sub>2</sub>O•••His513. This would promote the oxidation of linoleic acid at C9 rather than C13 as described earlier. For this to happen, the  $\omega$ -end of the fatty acid would have to extend past Thr274. Lipoxygenase-1 has a network of strong hydrogen bonds, His248•••Glu256•••Asn534, at that location while in lipoxygenase-3 this network is replaced by a water-bridged interaction, His266•••H<sub>2</sub>O•••Asp553, opening up enough space to accommodate the aliphatic substituent. Another sequence difference, Thr756/Arg775, controls the turn of the helix that includes Leu773, replacing a strong OG1Thr756•••OAsp752 interaction in lipoxygenase-1 with a large loop held in place by a Glu771•••Arg775 salt bridge in lipoxygenase-3. This combination of differences helps to explain why lipoxygenase-1 is more stringent, whereas lipoxygenase-3 allows for more options (C9/C13 and *R/S*). In this study, both stereoisomers were tested in the electron density maps. While the reaction of linoleic acid with lipoxygenase-1 produces 13-HPOD exclusively, a mixture of stereoisomers (*S/R*: 86/14) is obtained. Our crystals were soaked with the products of the lipoxygenase-1

reaction, and despite the abundance of 13(*S*), either stereoisomer could bind lipoxygenase-3, which produces nearly equal amounts of the two enantiomers. The discrepancy factors ( $R = 0.196$ ,  $R_{\text{free}} = 0.296$  vs  $R = 0.204$ ,  $R_{\text{free}} = 0.302$ ) came in favor of the *S* enantiomer.

The mode of binding observed in the crystal structure does not correspond to any of the previous predictions for substrate interactions based on molecular modeling using the native enzyme as a starting point.<sup>25</sup> An important point that has received considerable attention relates to the orientation of the substrate at the active site. Positional specificity has been attributed to either an orientation effect, i.e., the direction ( $\alpha \rightarrow \omega$  or the reverse) adopted by the fatty acid in the vicinity of the iron site, or a steric effect.<sup>25,26</sup> That is, the longer the hydrophobic pocket, the deeper the substrate might be able to penetrate, resulting in peroxidation farther away from the  $\omega$ -end. While the structure provides an explanation for the lack of regioselectivity in the reaction catalyzed by lipoxygenase-3 employing a variation of the latter hypothesis (vide supra), the possibility that fatty acid could bind in the head-to-tail reversed orientation cannot be ruled out. Further, the observations make it clear that a direct extrapolation to the situation in mammalian lipoxygenases cannot be made. For example, the hydrophobic pocket identified in the structure of soybean lipoxygenase-3 does not have a counterpart in the rabbit 15-lipoxygenase on the basis of sequence alignment alone. Further, the residues found consistently to influence positional specificity in the mammalian enzymes on the basis of site directed mutagenesis are not in positions to play similar roles in the fatty acid interaction in the lipoxygenase-3 structure. For example, residues Phe353, Ile418, and Ile593 in the sequence of rabbit 15-lipoxygenase have been implicated in the formation of the hydrophobic pocket that accepts the  $\omega$ -end of the fatty acid.<sup>26</sup> Phe353 in the rabbit sequence corresponds to Ser510 in the lipoxygenase-3 sequence (not an aromatic residue), and Ser510 is close to the place where the carboxylate group of 13-HPOD binds in the structure of the complex. It therefore seems increasingly likely that the determinants of regioselectivity and stereoselectivity in plant and animal lipoxygenases will turn out to be different.

**The Catalyzed Reaction.** It has been proposed that the purple species constitutes one of the intermediates in the lipoxygenase-catalyzed reaction, and the existence of the iron(III)–peroxide complex confirmed by the elucidation of its structure certainly supports this hypothesis.<sup>17</sup> A mechanism that includes the salient features of the catalytic cycle is provided in Scheme 1. Once the substrate combines with the iron(III) enzyme, a hydrogen atom abstraction takes place by a tunneling mechanism.<sup>4</sup> Transfer of the electron to the metal produces iron(II), while the proton acceptor is probably a hydroxide ligand on the iron. This chemistry leaves the fatty acid in the form of a free radical possibly either allylic or pentadienyl.<sup>27,28</sup> The radical combines with molecular oxygen under steric restraints that govern the stereoselectivity.<sup>24</sup> Combination of the peroxy radical intermediate with the iron(II) cofactor would produce the iron–peroxide complex. Dissociation of the peroxide with proton transfer would produce the product of the reaction and regenerate the starting iron(III) form of the enzyme. Invoking the iron–peroxide complex as an intermediate provides a logical route for the reduction of the peroxy radical intermediate.

(25) Prigge, S. T.; Boyington, J. C.; Gaffney, B. J.; Amzel, L. M. *Proteins Struct. Funct. Genet.* **1996**, *24*, 275–291.

(26) Kuhn, H. *Prostag. Lipid Mediat.* **2000**, *62*, 255–270.

(27) Nelson, M. J.; Cowling, R. A.; Seitz, S. P. *Biochemistry* **1994**, *33*, 4966–4973.

(28) Funk, M. O.; Andre, J. C.; Otsuki, T. *Biochemistry* **1987**, *26*, 6880–6884.

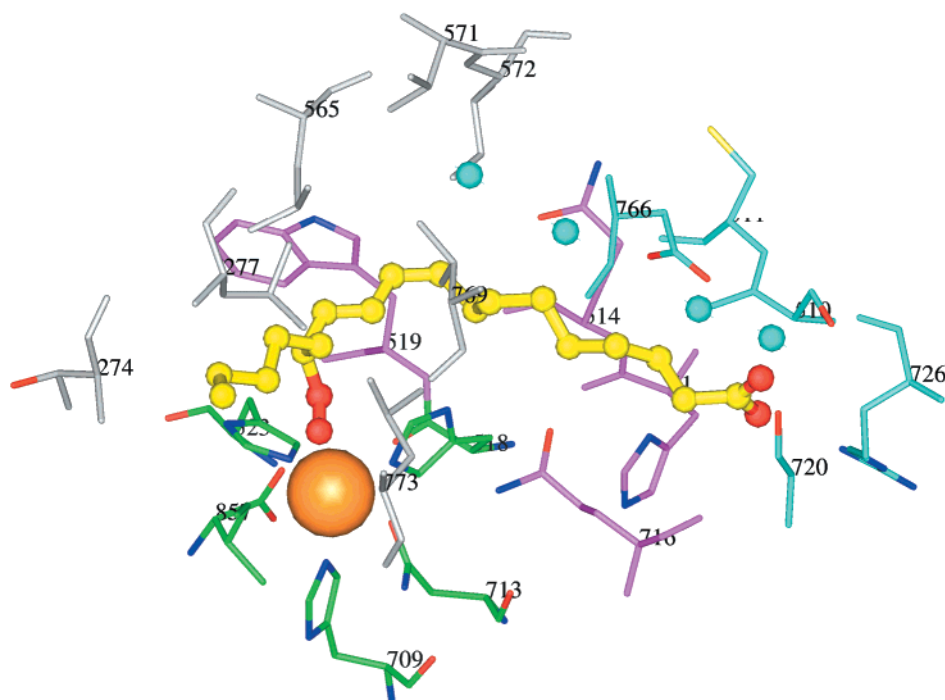


**Figure 4.** Binding of 13-HPOD (yellow) to soybean lipoxygenase-3. Amino acids are shown as follows: green, His 518, 523, 709, Asn 713, and Ile 857; purple, Trp 519, Gln 514, His 513, Gln 716; light blue, water molecules and Asp 766, Cys 511, Ser 510, Arg 726, and Gly 720; and gray, hydrophobic residues Ile 557, Leu 277, Leu 565, Val 571, Ile 572, Val 769, and Leu 773.

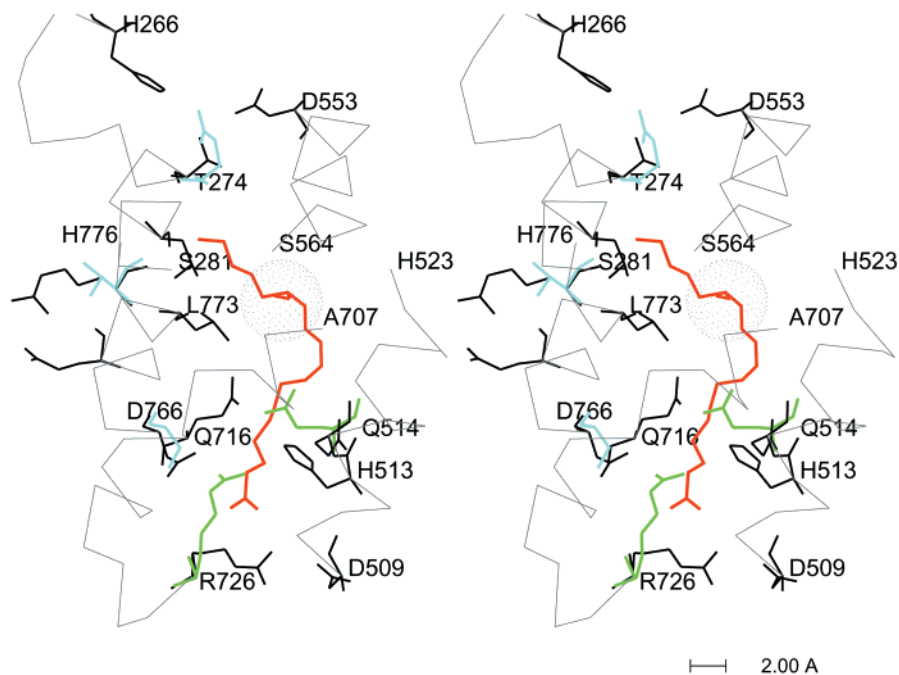


**Figure 5.** Features of the 13-HPOD binding site relevant to regio- and stereoselectivity. Selected residues in lipoxygenase-3 are black, the C $\alpha$  traces are thin gray lines with the ends indicated, the iron atom is a dotted sphere, and 13-HPOD is red. Corresponding residues in lipoxygenase-1 are in blue for comparison. The position of Gln 514 in the native enzyme and the alternative rotomer for Arg 726 are in green.

While the conformation of lipoxygenase-3 undergoes remarkably little change in the transition from the native state to the oxidized purple form, there are two noteworthy features of residues found in the fatty acid binding site (Figure 6). The central part of the product molecule, C9–C13, is near iron in a nonbonding distance. However, the electron density around the His 518 ligand indicates the capacity for the side chain to turn on an axis that passes through the imidazole ring bringing it close to C8 and C11 on one side of the fatty acid. On the other side of the molecule, Trp 519 can approach C9, C10, and C12 by a reorientation of the side chain involving a 180° flip

and 42° swing that maintains the original plane of the indole ring. These two residues therefore might be involved in the formation or stabilization of radical(s) via proton and/or electron transfer.

### Experimental Section

Lipoxygenase-3 was obtained from soybean seeds (Resnick) by using a chromatofocusing procedure.<sup>29</sup> UV–visible absorbance spectra were obtained on 250  $\mu$ M solutions of the enzyme at pH 8.5 (0.1 M TrisHCl). The 13-HPOD<sup>30</sup> was added as an aliquot ( $\leq 2.5\%$  of the total volume) in methanol to provide the appropriate ratio. EPR samples were prepared



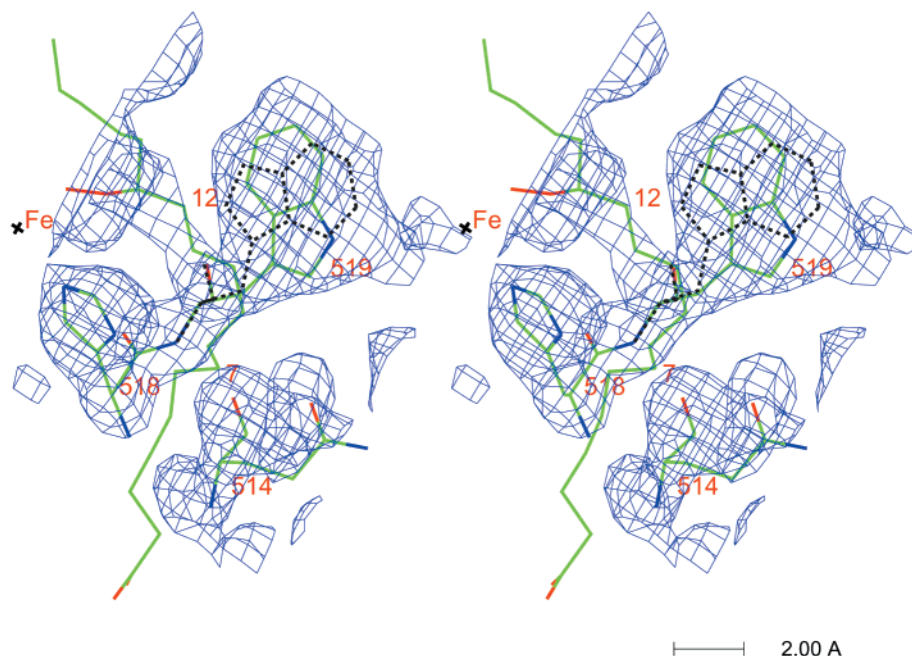


**Figure 6.** Unusual features of amino acids in the 13-HPOD bindings site.  $2F_o - F_c$  map showing a rounded shape for His518 and a flat but expanded shape for Trp519. The dashed line illustrates alternative conformation for tryptophan. 13-HPOD is in green.

by first transferring an appropriate aliquot of 13-HPOD solution in methanol to a plastic tube. The methanol was removed with use of a stream of nitrogen. The enzyme (0.25 mL, 250  $\mu$ M, pH 8.5, 0.1 M TrisHCl) was added to the tube, and the mixture was allowed to stand at room temperature for 10 min before being transferred to a quartz tube for freezing in liquid nitrogen. EPR spectroscopy was conducted on the frozen solutions as previously described.<sup>31</sup> The 9 GHz measurements were performed with a Varian Century Line Spectrometer equipped with a homemade, gas-phase liquid helium transfer line and quartz dewar cavity insert operating at 25 K.

Crystals of soybean lipoxygenase-3 were obtained from sodium citrate-phosphate buffer<sup>32</sup> and poly(ethylene glycol), MW = 8000, using the previously described protocol.<sup>7</sup> An ethanol solution of 13-HPOD was added to freshly prepared crystals of soybean lipoxygenase-3 in a 1:2 molar ratio (13-HPOD was tested in ratios of 1 to 15) with lipoxygenase-3. The concentration of ethanol did not exceed 1% of the total volume. The crystals slowly developed a purple color that vanished with time and exposure to light. The crystals were kept in an incubator at 23 °C in the dark and were used within 2 days. Exposure of the purple crystals to the microscope light during mounting and alignment was limited as much as possible. Crystals were placed in  $\phi$ 1 mm capillaries and data were collected at room temperature on RaxisIV with Cu rotating anode and focusing mirrors, at 50 kV, 100 mA, crystal-to-detector distance 140 mm, oscillation angle 2°, and exposure time 10 min per frame. The purple color of the crystals declines with time in the X-ray beam, so visual evaluation was made to estimate the time of total exposure per crystal that would correspond to the "purple" phase. In addition, an extremely conservative approach was taken in selecting the diffraction data. Forty frames corresponding to an 80° sweep of reciprocal space were collected for each crystal. After 6 h, the intensities had dropped to around 50%. Even though the purple color was still clearly visible at that point, we elected to cut the data at most at 80% intensity decay and combine reflections from three crystals to ensure the desired level of completeness, and to use data that corresponded to the purple phase. Only 20, 9, and 7 frames were used from crystals 1, 2, and 3, respectively. That corresponded to 3 h or less of data collection and decays in the intensity of 80%, 87%, and 90%. Data for the crystals were collected in the dark, and 107 634

observations from the three crystals were merged together yielding 48 693 reflections with 78% completeness to 2.0 Å resolution (68.4% in the 2.07–2.00 Å last shell) with  $R_{\text{merge}}$  6.4% based on intensities.<sup>33</sup> The unit cell dimensions for the crystals soaked with 13-HPOD,  $a = 112.6$  Å,  $b = 137.3$  Å,  $c = 61.89$  Å, and  $\beta = 95.6^\circ$ , were within 0.1–0.2 Å and the same C2 space group as the native crystals. The structure was solved by molecular replacement with native lipoxygenase-3 (PDB code 1LNH) as a model, 8–3 Å data, and followed by rigid body refinement for the whole molecule first and 5 domains later. Maps:  $2F_o - F_c$  and  $\Delta F$  calculated at this point ( $R = 0.25$ ) clearly showed an extended shape of an unoccupied density that could accommodate 13-HPOD. The protein molecule was examined against the maps and adjusted accordingly. Topology and parameter files for 13-HPOD were generated with "xplo2d"<sup>34</sup> and the parameters corresponding to similar structural features. All calculations were done in X-PLOR version 3.85<sup>35</sup> with  $R_{\text{free}}$  for 10% sampling of reflections for validation. All modeling and visual examinations after each round of refinement were performed with CHAIN version 7.<sup>36</sup> After including 13-HPOD into the calculations the structure was refined to  $R = 0.22$ ,  $R_{\text{free}} = 0.31$ , with 28 784 reflections in the 8–2.2 Å resolution range. Bulk solvent correction was introduced and the resolution range expanded to 40.0–2.0 Å, and solvent molecules were added gradually. Different configurations of the fatty acid were tested at the final stage. The reported model, refined against 41 035 observations (within 40.0–2.0 Å, with  $F > 2\sigma$ ) has a crystallographic  $R$ -factor of 0.196,  $R_{\text{free}}$  of 0.296, and consists of 7249 atoms: 6697 from 836 out of 857 protein amino acids (residues 1–8 and 33–45 were not included), one Fe(III) cofactor, 22 atoms of 13-HPOD, and 529 water molecules. The coordinates were deposited in the Protein Data Bank, code 1IK3.

**Acknowledgment.** E.S.-J. thanks Gerard J. Kleywegt for helpful discussions during the refinement procedure. This research was supported financially by the National Institutes of Health (GM 62140).

JA011759T

(29) Funk, M. O.; Carroll, R. T.; Thompson, J. F.; Dunham, W. R. *Plant Physiol.* **1986**, *82*, 1139–1144.

(30) Funk, M. O.; Isaac, R.; Porter, N. A. *Lipids* **1976**, *11*, 113–117.

(31) Draheim, J. E.; Carroll, R. T.; McNemar, T. B.; Dunham, W. R.; Sands, R. H.; Funk, M. O. *Arch. Biochem. Biophys.* **1989**, *269*, 208–218.

(32) Gomori, G. *Methods Enzymol.* **1955**, *1*, 138–146.

(33) Otwinowski, Z.; Minor, W. *Methods Enzymol.* **1997**, *276*, 307–326.

(34) Kleywegt, J. G. *CCP4/ESF-EACBM Newsletter Protein Crystallog.* **1995**, *31*, 45–50.

(35) Brünger, A. T. *X-PLOR ver.3.1: A system for X-ray crystallography and NMR*; Yale University Press: New Haven, Connecticut, 1993.

(36) Sack, J. S. *J. Mol. Graphics* **1988**, *6*, 224–225.

(37) Shindyalov, I. N.; Boume, P. E. *Protein Engineering* **1988**, *11*, 739–747.